Automating concept-drift detection by self-evaluating predictive model degradation

Trapped vortex cell for aeronautical applications: flow analysis through PIV and Wavelet transform tools

Salvatore Sedda[1], Costantino Sardu [1], Davide Lasagna[2], Gaetano Iuso[1,*]
Raffaele S. Donelli[3], Fabrizio De Gregorio[3]

[1]Department of Mechanical and Aerospace Engineering, Politecnico di Torino, Torino, Italy
[2]Engineering and Environment, University of Southampton, Southampton, UK
[3]Italian Aerospace Research Centre (CIRA), Capua, Italy
*corresponding author: gaetano.iuso@polito.it

Abstract Results of the application of a trapped vortex cell to an airfoil with the aim of improving the aerodynamic performances are presented for two complementary experiments arranged at CIRA and at Politecnico di Torino. In the CIRA experiments, PIV measurements on a simplified configuration were carried out to characterize the trapped vortical structure and its effect on the separating flow downstream of the cell. In the experimental investigation at Politecnico di Torino, static pressure distributions were measured around a complete airfoil model, to yield lift and pitching moment coefficients. Wake surveys were also carried out to measure the drag. To study the unsteady phenomena inside the cavity pressure fluctuations signals were also investigated using Kulite sensors. In both experiments, the angle of attack of the airfoil and the Reynolds number were varied. It is shown that the flow inside the cell is highly unsteady with significant shedding of flow structures downstream. This phenomenon results in a large region of separated flow, in higher drag and lower lift. By contrast, the cell flow is considerably stabilized and regularized by applying distributed suction over the cell wall. As a result, the flow downstream of the cell reattaches and lower drag and larger lift are observed.
Keywords: Trapped vortex cell, flow control, PIV

1 Introduction

A trapped vortex cell (TVC) is a cavity with a suitably designed shape that can be mounted on the suction side of airfoil to improve its aerodynamic performances. The idea of trapping vortices was probably first proposed by Ringleb [1]. Kasper [2] observed for his glider, in specific circumstances, higher lift, that he attributed to a trapped structure. The same idea was successively exploited by Savitsky and collaborators [3] who developed and tested in flight the EKIP, an aircraft equipped with several TVCs, distributed on the suction side of the aircraft.
Several investigations on the TVC technique were then conducted under the 6th framework EU project called VortexCell2050, with the focus of developing fundamental understanding. The experiments discussed in this paper were carried out under this project. Hokpunna and Manhart [4] studied the TVC flow by means of large eddy simulations. They identified four important flow regions inside and around the cell: the shear layer above the cavity, the stagnation region, the vortex core inside the cavity and the boundary layer along the wall cavity. Furthermore, they observed a spanwise modulation of the flow, which was also identified in an experimental investigation by Savelsberg and Castro [5]. Tutty et al. [6] showed that this modulation arises from the existence of a steady perturbation of the vortical flow. In an effort to develop fast and accurate simulation tools for rapid optimisation of the cavity shape, Donelli et al. [7, and 10], considered two-dimensional flows only. They concluded that RANS models were well represented by simpler Prandtl-Batchelor-type flow models, and that the RANS simulation matched quite well experimental data from a TVC airfoil-like configuration. One critical aspect of this geometry is that the vortex in the cell can be unstable and can escape from it or fail to develop properly. This problem was investigated by several authors. Chernyshenko [8] using the Föppl model demonstrated that superposition of oscillations can stabilize trapped vortex. Bouferrouk and Chernyshenko [9] performed an active stabilization control of a trapped vortex. These authors used suction inside the cavity and were able to improve the aerodynamic characteristics of a Lighthill's airfoil reducing the drag and increasing the lift. De Gregorio and Fraioli [11] showed by PIV measurement distributed suction on the cell wall can stabilise a coherent steady vortex inside a TVC mounted on the suction side of an airfoil-like configuration. Olsman and Colonious [12] studied the interaction between the cavity flow and the external flow using 2D direct numerical simulation. These

authors showed the existence of different modes of oscillation of the shear layer. Furthermore, the structures generated from the cell and released downstream of it were able to delay the separation.
The fundamental control mechanism is the "moving wall" effect proposed by Donelli et al. [13], whereby the boundary layer flowing over the cavity opening is, downstream of it, fuller and less prone to separate than in the case the cell is replaced by a solid wall. Separation delay then results in lower pressure drag and higher lift. Lasagna et al. [14] observed, through an experimental investigation performed on a thick airfoil, that the wing with the TVC produced more lift and less drag than the baseline wing. Furthermore, the performance was even better with respect to applying distributed suction on part of the baseline geometry. Following the ideas of Donelli [13], the authors argued that a coherent and stable vortex trapped inside the cell could originate a "moving wall" effect, producing higher momentum in the near-wall region downstream of the cavity.
Low Reynolds number applications of TVCs for flow control have been also reported. For example Shi et al. [15] showed that a TVC mounted on a thick NACA0020 airfoil typically worsened the performances at R_e=5000, from low to high angles of attack. A different application of TVCs at low Reynolds number is that reported by Mariotti et al. [16]. The author discussed the effects of trapped vortices to delay the flow separation in a divergent channel, showing a superior efficiency and smaller recirculation regions.
Results of PIV measurements performed at CIRA on a simplified airfoil-like configuration hosting 1 TVC are reported first. These highlight the variation of the flow structure when suction inside the cell is activated. Results of force coefficients measurements obtained at the Politecnico di Torino (PoliTo) are then reported to illustrate the effectiveness of the proposed flow control technique. In addition, wavelet analysis of wall-pressure fluctuations in the cavity region is reported.

2 Basic Experiment at CIRA

Basic studies on flow control require a large amount of experimental work that cannot be performed in a large and expensive wind tunnel. For this reason the CIRA CT-1 wind tunnel was selected for investigating the influence of several parameters on the effectiveness of the TVC system. The CT-1 is an Eiffel type open circuit wind tunnel. The maximum velocity achievable in the test section is 55 m/s with an accuracy of ±0.2%. The characteristic Reynolds number per unit length, relative to a test section velocity of 50 m/s is about $3.5 \cdot 10^6$. The typical turbulence level in the test section is less than 0.1%. The CT-1 test section is fully transparent allowing flow visualization and optical measurement methods.

2.1 Test Article

The aim of the research project was to investigate the capability of trapped vortex cells to control flow separation on thick airfoils. The phenomena were simulated by a devoted test-bed, which only partially reproduces a real airfoil flow but includes the main physical features responsible of flow separation. The test-bed (Fig.1) consisted of a thick airfoil characterized by a chord length of 350 mm and a spanwise length of 305 mm, whose lower part was removed.

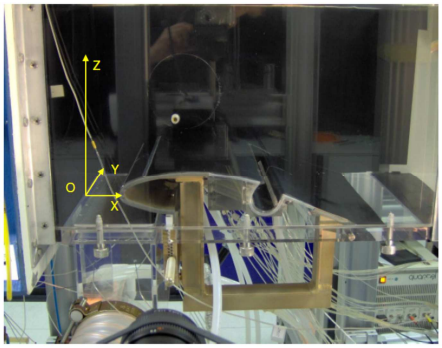

Fig. 1 - Test-Bed model and TVC drawer.

The test article was accommodated on the bottom wall of the wind tunnel section, hinged at the trailing edge and equipped with an adjustable guide on the lower side in the leading edge region. Such mechanism

allowed the rotation of the airfoil around the trailing edge varying the incidence angle between 5.66° to 12.66° with a step of 1°. The airfoil upper side was equipped with a removable drawer allowing the testing of different flow control devices. The drawer chordwise position was between x/c=0.36 and x/c=0.80. The TVC was located from x/c=0.59 to x/c=0.68. Controlled mass flow suction and/or flow blowing were applied inside the TVC. The model was equipped with 37 pressure taps (PTS), 33 PTS were longitudinal spaced and 4 PTS were spanwise located inside the TVC. The cavity was instrumented by 15 PTS in order to monitor the behavior of the vortex flow. The model geometry induced intense flow instability between the leading edge and the bottom WT wall due to the formation of an intense re-circulating zone. In order to confine/eliminate the circulation zone and neglect vortex shedding along the model, steady flow suction was applied in front the test article, in concomitance of the circulation region.

2.2 Measurement instrumentation

The values of the pressure taps located on the model test-bed and the static pressure in the test section upstream the model were acquired by means of the Hyscan 2000 system. Pressure taps were connected to a Scanivalve ZOC 22B electronic pressure scanner, characterized by full scale range of ±1 psi and accuracy value of ± 0.15% F.S.

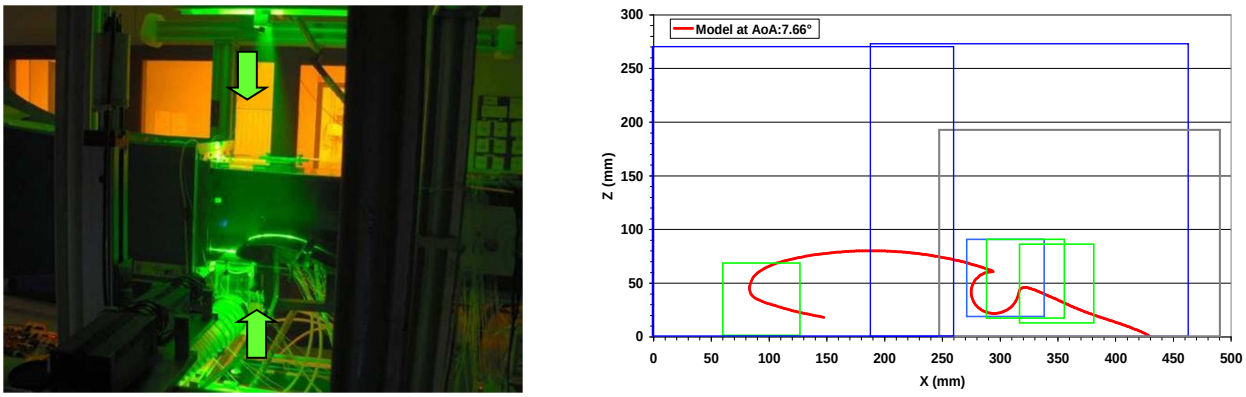

a) b)

Fig. 2 - Illumination system (a) and Model geometry with PIV recording regions (b).

Flow field measurements were carried out by means of a two components Particle Image Velocimetry system. The recording region was illuminated by two Nd-Yag resonator heads, each providing a laser beam energy of about 300mJ @ 532 nm. In order to measure simultaneously the upper and lower region of the model, in particular the flow field trapped between the model leading edge and the wind tunnel bottom wall and the flow inside the cavity, a double light sheet configuration was adopted (Fig. 2a). The investigation of the TVC flow behavior drove to measure the flow velocity inside the cavity. One of the difficulties coming from the experimental set up was optical access to the cavity. The TVC shape presented two main problems: absence of optical access, solved by building the cavity model by transparent material, and strong reflection due to the convex shape solved illuminating the cavity passing through the model bottom minimizing the reflection on the cavity surface. Different flow regions were simultaneously recorded by using two high resolution cameras (2048x2048 px) with different focal lens. A larger flow field (size: 270x270 mm2) with spatial resolution of 2.1 mm/vector aimed to provide a global overview of the flow velocity (blue and grey larger regions in Fig. 2b) A smaller field of view directed to measure the flow field below the model leading edge and the flow inside the cavity with a better spatial resolution of 0.5 mm/vector (smaller green and blue regions in Fig. 2b).

2.3 Test description

The tests were aimed to investigate the capacity of the TVC system to induce flow reattachment on the thick airfoil with either the application of flow suction inside the cell or not. The first step was to investigate the flow field behavior of the clean airfoil that was taken as baseline configuration. Different wind tunnel speed

(V=15 and 30 m/s) and incidence angle were tested (AoA=5.66°, 6.66°, 7.66°, 9.66°, 10.66° and 12.66°) in order to measure the flow separation points. The second step was the investigation of the airfoil equipped with the TVC without energy consumption, i.e. without flow suction for the same condition of speed and angle of attack. The last step was the investigation of the flow behavior under different conditions of flow suction for a limited set of speed and angle of attack values.

3 Wind tunnel investigation at PoliTo

The second experiment was carried out in the closed circuit subsonic wind tunnel at Politecnico di Torino. The test section has a circular shape with diameter and length equal respectively to 3 and 5 meters. A wing model having span equal to 1.2 m and chord *c* equal to 0.5 m was mounted between two end plates. The cross section of the wing was a NACA 0024 profile. The cavity extended from x/c=0.58 to x/c=0.71 with an opening length L=60 mm and a span b=400 mm resulting in an aspect ratio b/L=6.66. The shape of the curved cavity was designed by Chernyshenko et al. [17] using the Prandtl–Batchelor flow model.
Measurements of pressure distributions around the airfoil were performed to evaluate the lift and the pitching moment. Wake analysis were carried out using a rake equipped with 44 total pressure probes and 3 static pressure probes. It was located two chords downstream of the airfoil trailing edge. Pressure fluctuations were measured by means of five XCS-093 Kulite pressure transducers positioned inside and just outside the cavity. In figure 3a and 3b are respectively reported the front view of the model in the test section and the module with the trapped vortex cavity. In figure 3b the module that housed the cavity shows also the portion of the suction zone inside the cavity.

a) b)

Fig. 3 - The wing model and the module with the trapped vortex cell

4 Results

The most significant results obtained in the two experiments are presented in the following. The cases with the suction are characterized by a non-dimensional mass flow rate C_m defined as $\dot{m}\,V_s/qS$ where $\dot{m}$ is the mass flow rate, V_s the suction velocity, q the dynamic pressure of the undisturbed flow and S is the plan model surface.

4.1 CIRA results

The flow velocity time averaged velocity fields indicate for $\alpha = 7.66°$ a flow separation occurring at about x/c = 0.7 (Fig. 4a) whereas for the same incidence angle the model with the TVC installed shows flow separation at the cusp of the cavity at about x/c = 0.54 (Fig. 4b). The results indicate that without suction in the cavity, no positive influence of the TVC on the flow field, at least in terms of separation delaying was present. The same ineffectiveness was found at different wind tunnel speeds (from 15 to 30 m/s) and different incidence angles of the airfoil. In all the cases the flow field and the pressure coefficient show that the flow separates just upstream the cavity cusp and does not reattach. This effect was more pronounced as the wind speed or the airfoil rotation were increased. For this reason, the attention was focused on the lower velocity (15 m/s). The flow field behavior inside the cavity and immediately outside along the airfoil surface was investigated at wind tunnel speed of 15 m/s varying the angle of attack (Fig. 5a) A) α=5.66°, B) α=6.66°, C) α=7.66°, D) α=9.66°, E) α=10.66° and F) α=12.66°). The velocity magnitude color map and

the flow streamlines showed for the smallest angle a weak vortical structure inside the cavity, increasing the incidence angle the vortex center moved toward the shear layer region with the shape of the vortex stretching toward the exit of the cavity. The vortex strength was not sufficient to force the flow reattachment.

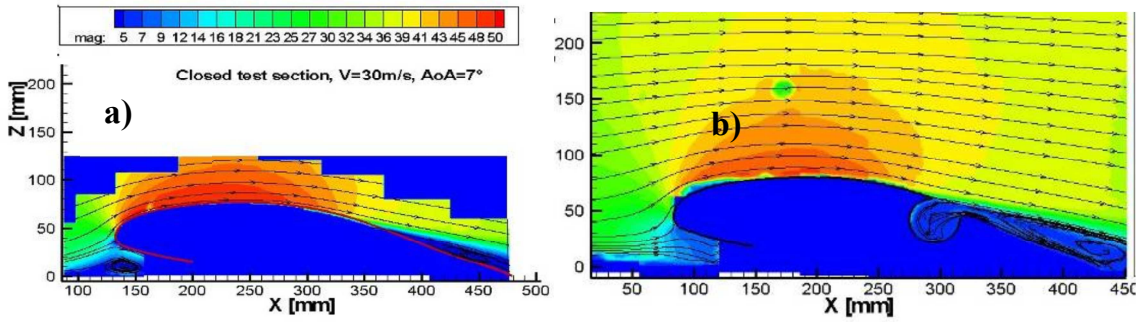

Fig. 4 - Flow field around baseline configuration (a) and passive TVC without suction (b)

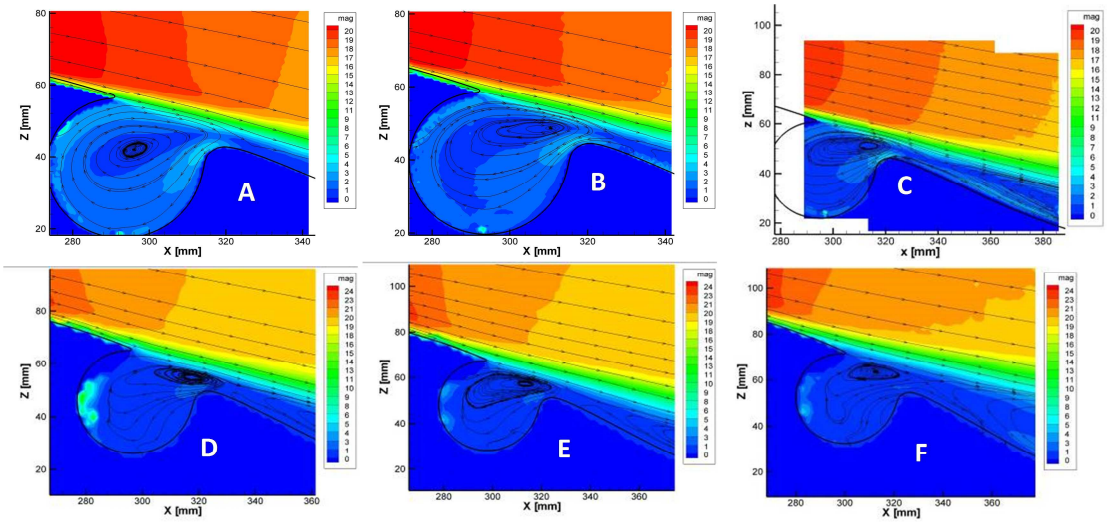

Fig. 5 - PIV-measured velocity field for several angles of attack. No-suction inside TVC. V=15m/s

The same behavior can be observed from the pressure coefficient distribution as a function of the incidence angle (Fig. 6). It is worth to stress that in this plot the pressure taps inside the cavity are located between x/c=0.54 and x/c=0.66. The pressure distributions show the typical behavior of flow separation, with a leading edge expansion followed by a pressure recovery region until reaching flow separation. An increment in the incidence angle moved the flow separation location upstream from the cavity cusp. This was assessed both by the flow field results as well as by the plateau region in the pressure distributions.

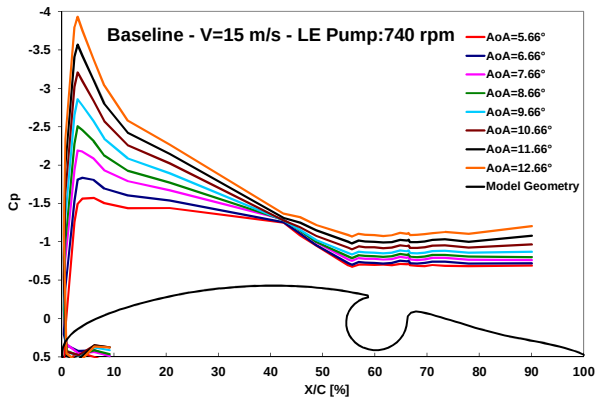

Fig. 6 - C_p distributions for several AoA. No-suction. V=15m/s

The results clearly indicated that TVC alone was not able to induce flow reattachment. In order to achieve this aim steady suction inside the cavity was applied. Different values of mass flow rates were tested for different incidences. Herein, only the cases related to a wind tunnel speed of 15 m/s, α=7.66° and homogeneous suction are discussed.
The flow behavior in the cavity was investigated for four different momentum coefficient: A) C_m =0.000189; B) C_m=0.000756; C) C_m =0.0021; D) and C_m =0.0059 (Fig. 7). The case A, characterized by the lowest value of C_m, showed little improvements if compared to the no-suction case (Fig. 4b). By increasing the suction to C_m =0.000756, a stable vortical structure is established inside the cavity. The vortex center is located almost in the geometrical center of the cavity and the flow is forced to reattach downstream, but it separates again at x/c=0.75. Further increasing the value of C_m, case C and D, the vortex is strengthened and it induces a full reattachment of the flow up to the end of the airfoil. This effect is clearly visible by the increment of the velocity magnitude in the cavity and by the streamline patterns. Confirmation of this is found in the behavior of the out of plane vorticity, that clearly indicated an increment of the vorticity from the case A to the case D.

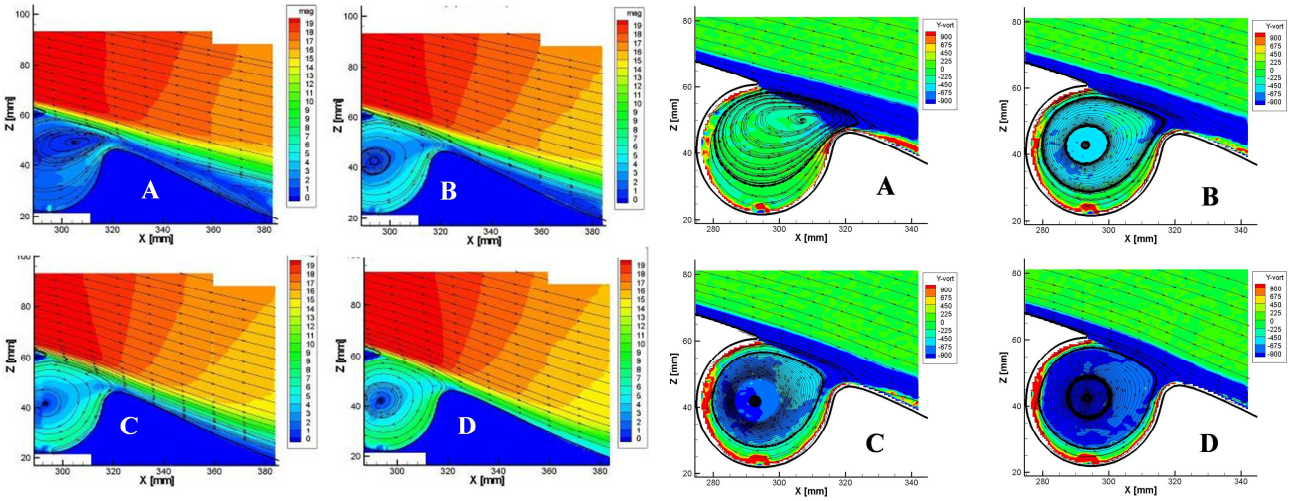

Fig. 7 - Velocity magnitude (left) and vorticity magnitude (right) varying flow suction. α=7.66° , V=15m/s

A comparison between the pressure coefficient distribution for the C_m =0 case and the case with C_m=0.000189 suggests that flow acceleration occurs immediately upstream the cavity, induced by the presence of the (weak) vortex (Fig. 8a). The higher (negative) C_P values in the cavity indicated an increment of the tangential flow velocity in the cavity. The C_P trend downstream the cavity showed no pressure recovery, indicating that the flow remained separated for this mass flow rate (MFR), as already shown by the PIV measurements.

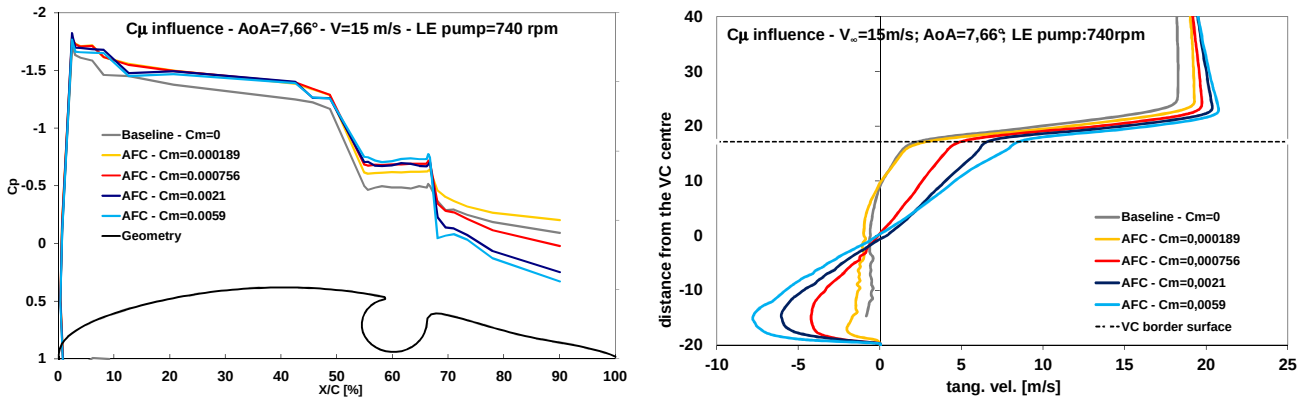

a) b)

Fig. 8 - Cp distributions varying Cm at V=15m/s (a) and tangential velocity inside the cavity varying Cm (b)

As the suction was increased to C_m=0.000756, the C_P behavior showed the same trend as before both upstream and in the cavity, but an increased downstream pressure recovery was visible, since the flow reattachment became appreciable. This tendency was more and more visible as the MFR increased, as was evident for the last two cases. It is worth noting that in the case with maximum suction (C_m=0.0059) the C_P in the cavity reaches its maximum negative value indicating a maximum of rotation (and tangential speed) of the trapped vortex. This was also confirmed (Fig. 8b) by the tangential component of the velocity plotted along the axes orthogonal to the shear layer boundary and passing from the flow vortex center. Moreover, as it can be observed from Fig. 8b diagram, except for the lower MFRs the experimental velocity profiles inside the cavity show an almost linear trend, indicating a region of constant vorticity in accordance with the Prandtl-Batchelor theory (*e.g.*, see Donelli *et al.* 2009) and its application to predict cavity flows.

4.2 PoliTo results

The investigation at Politecnico di Torino was focused on the evaluation of the flow suction effects on the wing performances varying the incidence and the Reynolds number. In the following some significant results for $R_e=10^6$ are reported. Figure 9 shows the comparison between the drag polar for the baseline, the passive cavity (C_m=0) and the cavity with suction (C_m=0.0012) for which a well coherent vortex is trapped in the cavity. This cavity flow organization is also shown in the basic experiment (Fig.7 case B and C) for which the values of C_m are in a range that include the current value. In figure 10, the lift to drag ratio as a function of the incidence angle are reported for the same cases. As it can be observed the performances of the airfoil increase considerably when the active flow control is applied. In contrast, without suction the drag increases while the lift decreases for all the incidence angles. The value of C_{Dmin} is reduced approximately by 50% in the case of active cavity respect to the baseline, while the C_{Lmax} increases of about 20%. The L/D ratio also increases and its maximum value is more than doubled for the cavity with suction. The cavity without flow control (C_m=0) exhibits the worst performances even respect to the baseline.

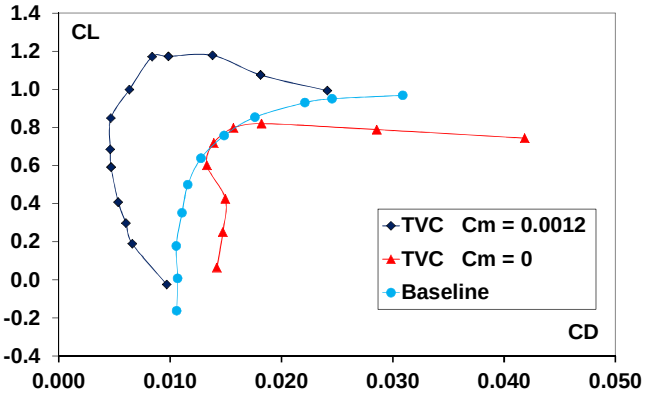

Fig. 9 - Drag polar comparison

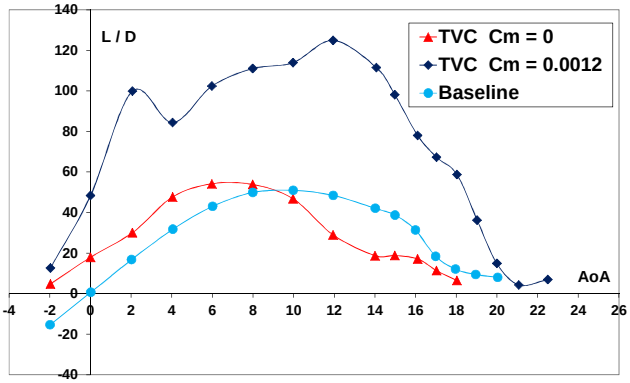

Fig. 10 - Lift to Drag ratio comparison

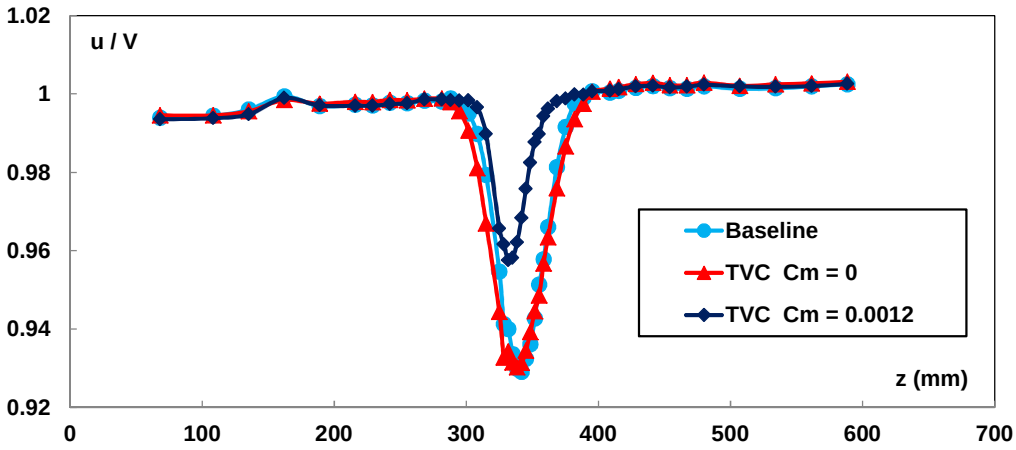

Fig. 11 - Wake velocity profiles at α=4°

The wake velocity distributions for the three configurations introduced before are reported in figure 11 for the incidence α=4°. Comparing the velocity profile of the airfoil with active cavity with those pertaining to the baseline and the passive cavity cases, a much lower momentum deficit in the wake of the airfoil with cavity respect to the others is noticeable. As reported in Lasagna et al. [14] and by previous PIV results, without control the trapped vortex inside the cavity is unstable in the sense that it is subject to escape from the cavity or to the intermittent breakdown originating early flow separation downstream the cavity. Such behavior is responsible of the reduced lift and increased drag. On the contrary when the suction is present the trapped vortex reside steadily in the cavity and originate at the interface of the cavity a " moving wall" as shown more in details in Lasagna et al. [14]. Such behavior strengthen the near wall flow in the reattachment region and as a consequence to the flow separation is delayed.
The unsteady aspects characterizing the flow inside the cavity are analyzed through the wavelet transform of the pressure fluctuation signals. These signals were sampled at a frequency equal to 8 kHz for a total of 2^{20} samples by means of 5 Kulite sensors located as displayed in figure 12.

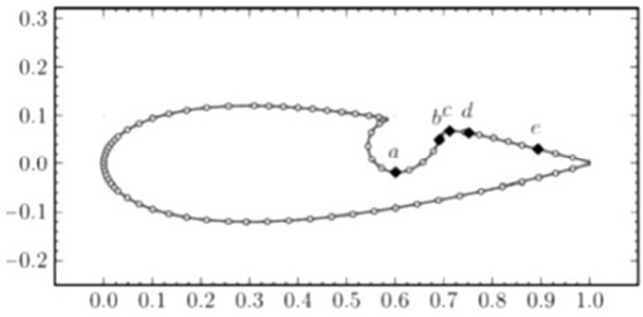

Fig. 12 - Kulite sensors locations

Results are presented in terms of wavelet energy density color maps that highlight the energy content simultaneously in frequency and time allowing to study the spectral components locally. Time and frequency have been made nondimensional using the free stream velocity and the cavity length. Due to representation issues, only the significant portion of the energy density map is displayed.
The signals of 3 significant sensors have been considered: the one in the lowest part of the cavity (***a***), the one close the flow reattachment region (***b***) and the one located in the reattached flow region where a boundary layer flow is present (***e***). In figure 13 and 14 the maps for sensor (***a***) and sensor (***b***) are reported respectively for the incidence α=4°. As it can be observed in figure 13 the energy distribution is mainly concentrated around a Strouhal number equal to 0.1 for all the observation time. This is associated to the characteristic wake mode of cavity flows which is related to the low frequency large scale vortex shedding.

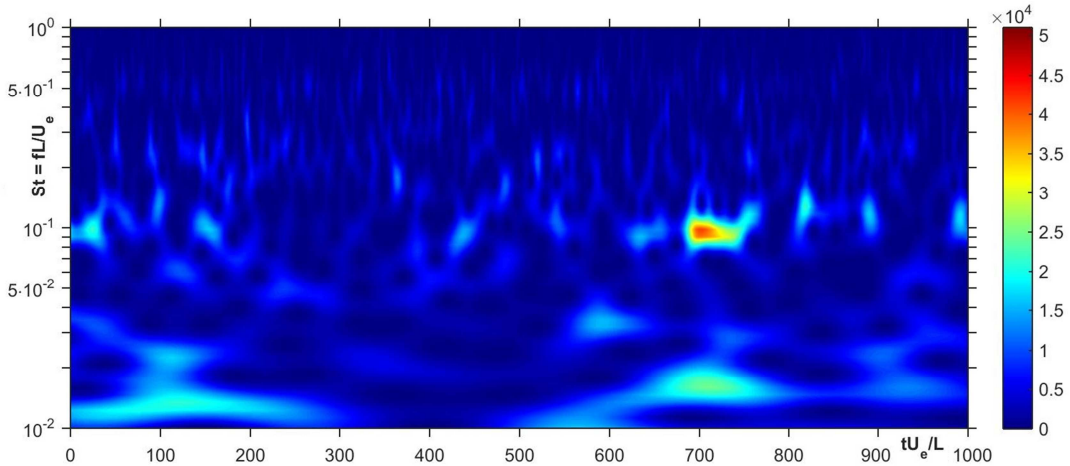

Fig. 13 – Wavelet energy density map. Kulite (***a***), C_m=0.0012 α=4°.

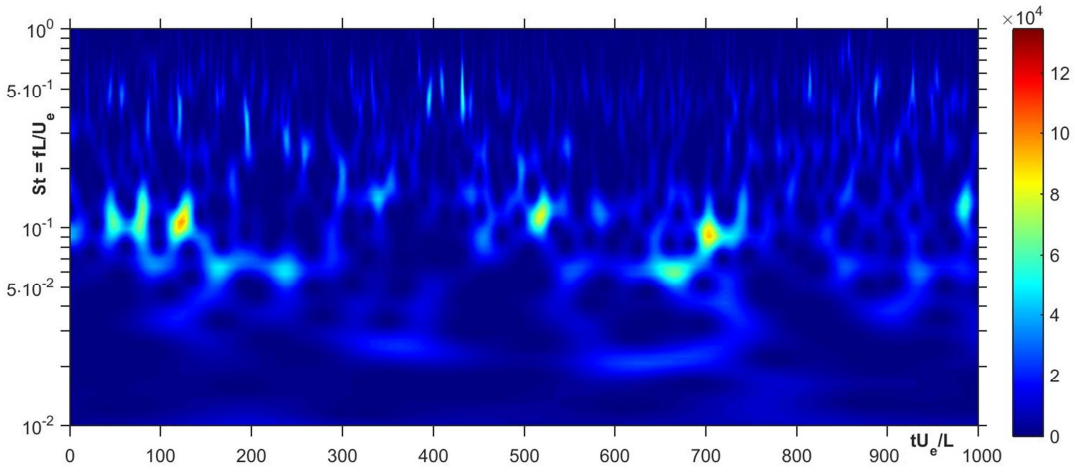

Fig. 14 - Wavelet energy density map. Kulite (***b***), C_m=0.0012. α=4°.

The energy density map relative to the sensor ***b*** in the reattachment region, reported in figure 14, shows two frequencies of energy concentration. The first corresponds to S_t=0.1 and represents the wake mode as in the previous case. The second one, instead, located around a Strouhal number equal to 0.6 pertains to another cavity flow behavior, namely the shear layer mode, which is linked to the shear layer instability generated at the upstream cusp of the cavity. These observations have been widely investigated in Lasagna et al. [14]. Finally, from figure 15, it is evident the weakening of the wake mode that still persist and at the same time a low frequency energy containing appears at around a Strouhal number in the range 0.01-0.02. These frequencies can probably due to the presence coherent structures typical of turbulent boundary layer developing on the wall of the airfoil.

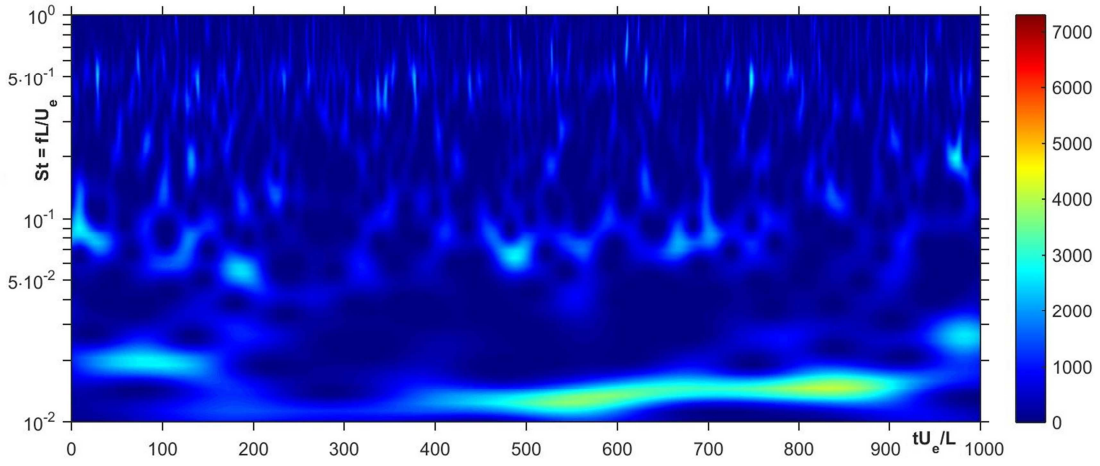

Fig. 15 - Wavelet energy density map. Kulite (***e***), C_m=0.0012. α=4°.

5 Conclusions

The flow behavior around an airfoil with an unconventional cavity positioned on the suction side has been investigated in two complementary experimental investigations. The cavity is able to trap a vortex inside that results stable only if appropriate values of the suction is present as shown by the PIV and the wind tunnel results. Without control the vortex is strongly unsteady and frequently escape from the cavity deteriorating the performances of the airfoil also respect to the baseline. In presence of the suction the trapped vortex cell determines an increasing of the C_{Lmax} of about 20% and a reduction around 50% respect to the baseline geometry. The effect of the stable vortex inside the cavity promote the presence of a flow in the near wall region downstream the cavity more resistant to the flow separation originating the improvement of the aerodynamic characteristics of the airfoil. From an applicative point of view an estimation of the energy

budget have to be evaluated. For the present experiment there was no optimization of the pneumatic line in order to reduce the power spent. Moreover also other lesser consuming energy flow control techniques can be used instead of the suction technique. Two typical unsteady cavity flow behaviors has been evidenced also for the present unconventional cavity, namely the shear layer and the wake mode characterized by a non-dimensional frequency around 1 and 0.1 respectively.

References

[1] Ringleb F.O. 1961. "Separation control by trapped vortices" In: Boundary Layer and Flow Control, Ed. Lachmann G.V., Pergamon Press
[2] Kasper W. (1974) "Aircraft wing with vortex generation". US Patent 3831885
[3] Savitsky, A. I., Schukin, L. N., Karelin, V. G. "Method for Q18 Control of the Boundary Layer on the Aerodynamic Surface of an Aircraft, and the Aircraft Provided with the Boundary Layer Control System" U.S. Patent No. 5417391, 23 May 1995.
[4] Hokpunna A. and Manhart M. "A large eddy simulation of a Vortex Cell flow with incoming turbulent boundary layer" International Journal of Mechanical Systems Science and Engineering 1;3 © www.waset.org Summer 2007
[5] Savelsberg R, Castro I. "Vortex flows in open cylindrical section cavities". Exp. Fluids (2008) 46(3):485–497
[6] Tutty O., Savelsberg R. and Castro I.P. "Three-dimensional flow in circular cavities of large spanwise aspect ratio." Journal of Fluid Mechanics 707 (2012): 551-574.
[7] Donelli R., Iannelli P., Chernyshenko S., Iollo A., and Zannetti L. "Flow Models for a Vortex Cell", AIAA Journal, Vol. 47, No. 2, pp. 451-467, (2009).
[8] Chernyshenko, S. I. "Stabilization of Trapped Vortices by Alternating Blowing-Suction" Physics of Fluids, Vol. 7, No. 4, 1995, pp. 802–807. doi:10.1063/1.868603
[9] Bouferrouk, A. and S.I. Chernyshenko "Stabilization of a trapped vortex for enhancing aerodynamic flows" 15th Australian Fluid Mechanics Conference, Sydney 13-17 December 2004, Australia
[10] Donelli R.S., De Gregorio F., Iannelli P. "Flow Separation Control by Trapped Vortex" AIAA 2010-1409, 48th AIAA Aerospace Sciences Meeting Including the New Horizons Forum and Aerospace Exposition, Orlando, Florida, January 4th -7th, 2010.
[11] De Gregorio F., Fraioli G. "Flow control on a high thickness airfoil by a trapped vortex cavity" 14th International Symposium on Applications of Laser Techniques to Fluid Mechanics, Lisbon, Portugal (2008)
[6] Olsman W.F.J., Colonius T."Numerical simulation of flow over an airfoil with a cavity" AIAA J 49:143–149 (2011)
[13] Donelli R., Chernyshenko S., Iannelli P., Iollo A., Zannetti L. "Flow models for a vortex cell" American Institute of Aeronautics and Astronautics, Paper 2(47):451–467 (2009)
[14] Lasagna D., Donelli R.S., De Gregorio F. and Iuso G. "Effects of a trapped cell on a thick wing airfoil" Exp.Fluids 51:1369–1384 DOI 10.1007/s00348-011-1160-9 (2011)
[15] Shi S., New T.H., and Liu Y. "On the flow behaviour of a vortex-trapping cavity NACA0020 aerofoil at ultra-low Reynolds number" 17th International Symposium on Applications of Laser Techniques to Fluid Mechanics, Lisbon, Portugal, 07-10 July, 2014
[16] Mariotti, A., Grozescu, A. N., Buresti, G., & Salvetti, M. V. "2Separation control and efficiency improvement in a 2D diffuser by means of contoured cavities". European Journal of Mechanics-B/Fluids, 41, 138-149. (2013)
[17] Chernyshenko S.I., Castro I.P., Hetsch T., Iollo A., Minisci E., Savelsberg R. "Vortex cell shape optimization for separation control" 5th European congress on computational methods in applied sciences and engineering (ECCOMAS 2008), Venice, Italy